

## Positronium Velocity Spectroscopy of the Electronic Density of States at a Metal Surface

A. P. Mills, Jr., Loren Pfeiffer, and P. M. Platzman

*Bell Laboratories, Murray Hill, New Jersey 07974*

(Received 10 June 1983)

The velocity of positronium (Ps) formed when 1–2-keV positrons are implanted into an Al(111) target and diffuse to the clean surface has been measured. The time-of-flight distribution exhibits a sharp step at a Ps energy 2.62(4) eV in excellent agreement with the expected Ps work function  $\varphi_{\text{Ps}} = -2.60(3)$  eV obtained from the known electron and positron work functions of Al(111). The presence of less than a monolayer of oxygen reduces the step amplitude by a factor of 2. It is shown that this spectrum is a measure of the surface density of states.

PACS numbers: 71.60.+z, 73.20.Cw

Since positronium (Ps) was first observed to be formed at metal surfaces in vacuum, its origin has been the subject of considerable interest.<sup>1</sup> Positrons ( $e^+$ ) implanted into a metal diffuse back to the surface where they are either trapped, emitted as slow  $e^+$  if the material has a negative positron work function, or emitted as Ps. If the metal is heated the  $e^+$  trapped at the surface may be thermally desorbed as Ps. Little is known about the directly emitted Ps except that it is "fast" (not thermal). If this fast Ps were formed adiabatically the metal would be left in its ground state and the Ps would have an energy equal to minus the Ps work function ( $-\varphi_{\text{Ps}}$ ) with a width given by the apparatus resolution and the thermal spread. Here  $-\varphi_{\text{Ps}}$  is equal to the Ps binding energy  $\frac{1}{2}R_\infty$  less the sum of the electron and positron work functions,  $-\varphi_{\text{Ps}} = \frac{1}{2}R_\infty - \varphi_- - \varphi_+$ . If the fast Ps forms suddenly the metal will be left in an excited state and the Ps energy spectrum will show a step extending from  $-\varphi_{\text{Ps}}$  toward lower energies. We report here the first measurements of the fast Ps velocity spectrum. The data show that the formation process is in fact sudden. Because of this, the data may be interpreted in terms of a very simple physical picture which implies that positronium velocity spectroscopy is a unique probe of the electronic density of states near the surface of a solid.

The Ps time-of-flight apparatus<sup>2</sup> is shown in Fig. 1. A beam of slow positrons was pulsed at 1 kHz to obtain 8-nsec full width at half maximum (FWHM) bursts each containing  $\sim 80$  positrons. The positron bursts were implanted into the sample at 1–2 keV, thus ensuring that most of the positrons thermalized before diffusing back to the surface where the Ps formation takes place. About 20 triplet Ps atoms formed at the sample surface after each burst, and expanded

into the vacuum chamber. The subsequent  $\gamma$  decay of the Ps was observed by a counter behind a movable slit located a distance  $z$  from the sample surface. The spatial resolution and the  $z = 0$  position were established by mapping the count rate versus  $z$ . The spatial resolution measured in this way was 3.9 mm FWHM. A collimator limited the Ps emission to within  $18^\circ$  of the forward direction. The 99.999% pure Al(111) sample was mounted perpendicular to the positron beam axis. It was prepared by bombardment with 1-keV  $\text{Ar}^+$  ions followed by annealing at  $630^\circ\text{C}$ , in UHV (base pressure  $3 \times 10^{-10}$  Torr). Ps thermal-activation measurements lead us to believe that the surface quality of our sample was comparable to that of previous samples that exhibited sharp low-energy electron-diffraction spots and less than 2% of a monolayer of O and C contamination.

The positronium time-of-flight data with the slit set at  $z_0 = 74 \pm 1$  mm are shown in Fig. 2 plotted on an energy scale given by  $E = m_e z_0^2 / t^2$ .

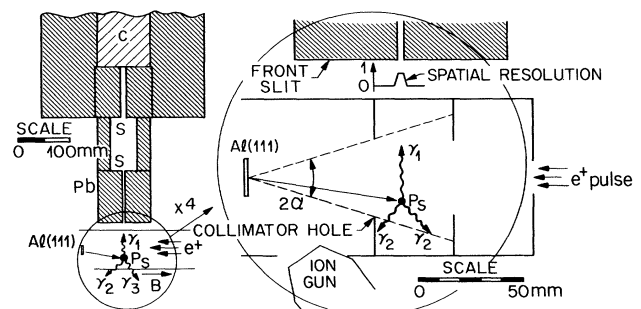


FIG. 1. Apparatus for measuring positronium velocities by time of flight. C,  $4 \times 8 \times 8$ -in.<sup>3</sup> plastic-scintillator  $\gamma$ -ray detector; Pb, 4-in.-thick lead shield; S, 6-mm- and 3-mm-wide lead slits; Ps, triplet positronium emitted from the Al(111) target; B, positron-beam-transport magnetic field;  $e^+$ , 8-nsec-FWHM burst of positrons about to hit the target.

The spectra were recorded on a multichannel analyzer using a time-to-amplitude converter started by the positron accelerator pulse and stopped by the detected  $\gamma$  ray. The prompt peak defines  $t=0$  as was established by a separate run with  $z=0$ . The background due to accidentals has been subtracted, and the data have been multiplied by  $\exp[t/(142 \text{ nsec})]$  to correct for the effect of triplet-positronium annihilation. The upper spectrum obtained with the clean Al(111) sample exhibits an abrupt count-rate increase at a positronium kinetic energy of about 2.6 eV indicated in the figure. The lower spectrum was obtained after exposing the clean Al sample to  $\sim 10^{-4}$  Torr sec of  $O_2$  which covers it with less than 1 monolayer of oxygen.<sup>3</sup> Now the step increase is much reduced. The curves shown in Figs. 2 and 4 are theoretical fits to be discussed below.

A simple physical picture along with a semi-quantitative estimate of the formation probability as a function of energy and momentum of the outgoing positronium is possible. As the thermalized positron approaches the vacuum it carries with it a correlated cloud of electrons. At low enough densities this cloud begins to resemble vacuum positronium, a bound state in the uniform gas<sup>4</sup> appearing at  $r_s = n^{-1/3} a_0 \approx 6$ , where  $a_0$

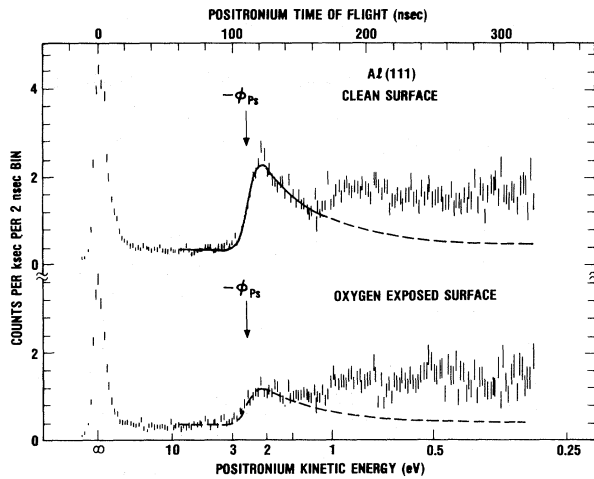


FIG. 2. Positronium time-of-flight spectra. The peaks at  $t=0$  are due to  $\gamma$  rays which originate from prompt positron annihilation and scatter into the slits. The asymmetry of these prompt peaks towards long delay times is due to scattering of the prompt  $\gamma$  rays through differing paths. The valley to the right of each prompt peak is due to scattered  $\gamma$  rays from the triplet positronium which decays before reaching the slits.

$\approx \hbar^2/me^2$ . This threshold electron density  $n$  is about 2.5% of the bulk density for Al( $r_s=2$ ). According to Lang and Kohn<sup>5</sup> this happens at a distance  $z_c=1.2 \text{ \AA}$  out from the sharp jellium background which is located half an interlayer spacing out from the last layer of atoms. This virtual Ps in the presence of the surface potential is liberated from the solid leaving behind the single hole required by charge conservation. The Feynman diagrams for this process are shown schematically in Fig. 3. The double open (shaded) line represents a bare (clothed) positron; the single lines, electrons (up) and holes (down); and the dashed line, a bare Coulomb interaction. All of the operators are understood to obey the boundary conditions imposed by the surface.

The differential rate (probability) for Ps emission from the metal is

$$dN \sim \sum_i d^3q |M_i|^2 n_i \delta(E_{\vec{q}} + (E_F - E_i) + \phi_{Ps}). \quad (1)$$

Here  $\vec{q}$  is the momentum of the Ps atom,  $n_i$  and  $E_i$  are the occupation number and energy of the  $i$ th electron, and the matrix element  $M_i$  is the infinite set of perturbation terms indicated in Fig. 3. A good approximation for the complete vertex  $V$  is a bare Coulomb interaction near the surface leading to the Ps bound state (see Fig. 3). In this case we may write

$$M_i = \int d^3x d^3X \psi_{Ps}^*(\vec{x}, \vec{X}) \frac{e^2}{|\vec{x} - \vec{X}|} \psi_p(\vec{X}) \psi_i(\vec{x}) = \int g(\vec{x}) \psi_i(\vec{x}) d^3x. \quad (2)$$

Here  $\vec{x}$  ( $\vec{X}$ ) is the coordinate of the electron (positron), and  $\psi_i(\vec{x})$ ,  $\psi_{Ps}(\vec{x}, \vec{X})$ , and  $\psi_p(\vec{X})$  are the electron, positronium, and fully clothed positron wave functions in the presence of the surface.

In order to evaluate Eq. (2) precisely we may use band-structure calculations of  $\psi_i$  and  $\psi_p$ , the vacuum Ps wave function, and the bare Coulomb interaction. However, we can make additional progress in understanding the qualitative behavior of Eq. (2) without going into any of these details. The function  $g(\vec{x})$  defined by Eq. (2) is

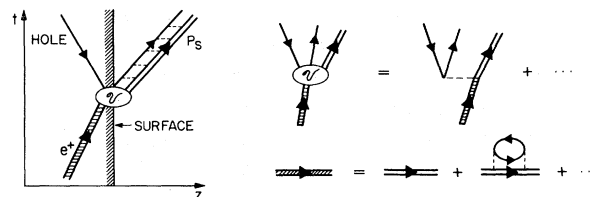


FIG. 3. Feynman diagrams for positronium emission from a surface.

peaked near  $z_c$  with a width approximately equal to the Ps Bohr orbit. For a surface with translational symmetry parallel to the vacuum interface  $\sum_i = \sum_j \int d^2 k_{\parallel}$  and

$$g(\vec{x}) = g(z) \exp(i\vec{q}_{\parallel} \cdot \vec{x}_{\parallel}). \quad (3)$$

It is important to note that  $g(z)$  contains all of the information about the matrix element and the overlap connected with the internal Ps wave function. We may then write

$$dN \sim \sum_j d^3 q n_j(\vec{q}_{\parallel}) |\psi_i(\bar{z} + z_c)|^2 \delta(E_{\vec{q}} + [E_F - E_j(\vec{q}_{\parallel})] + \varphi_{Ps}). \quad (4)$$

Although the precise value of  $\bar{z}$  in Eq. (4) is determined by the details of the electronic band structure and the exact form of  $g(z)$ , we know from our above argument that  $\bar{z} \approx 1 \text{ \AA}$ . To use this expression for a comparison with experiment it must be integrated over the acceptance solid angle of the collimator,  $\int d^2 q_{\parallel}$ . In general the integral cannot be simply evaluated. However, if the collimator keeps  $q_{\parallel}$  small (typically  $q_{\parallel} \ll k_F$ ) then  $E_j(q_{\parallel}) = E_j(0)$  and the angular part of the  $q$  integration except for a small region near  $E_q = |\varphi_{Ps}|$  can be done; i.e.,

$$dN/dE_{\perp} \sim E_{\perp}^{1/2} \sum_j |\psi_i(\bar{z} + z_c)|^2 \delta(E_{\perp} + (E_F - E_j) + \varphi_{Ps}) = E_{\perp}^{1/2} \rho_s(E_{\perp}). \quad (5)$$

The Ps yield is thus proportional to a density of states centered around a distance approximately  $1 \text{ \AA}$  outside the metal surface but averaged over a region about the size ( $1 \text{ \AA}$ ) of the positronium atom. This one-electron pickup is reminiscent of the two-hole Auger process in ion neutralization spectroscopy.<sup>6</sup> In both cases the electron falls into a bound state leaving a hole in the Fermi sea. As a result of the heavy mass of the ion, the difference in energy must be given to an electron-hole pair (the Auger electron) in the solid. In our case, because of the light Ps mass the excess energy may be taken up by the center-of-mass motion of the Ps. Higher-order processes involving additional electron-hole pairs can also occur. The importance of these processes is very similar to the importance of mul-

tipole-hole states in x-ray photoemission spectra. In the latter case the outgoing electron has such high energy that there is minimal shakeup due to its interaction with the remaining electrons. The positronium is formed in the tails of the electron density and once formed is neutral so that there is little residual Coulomb interaction between it and the remaining electrons. Both processes are modified by shakeup on the hole. A variety of experimental results indicate that such effects contribute at the 10% level.<sup>7</sup>

For a free-electron metal like Al,  $E_i = \hbar^2 k_i^2 / 2m$ . In addition if we set  $|\psi_i|^2 = \text{const}$ , which is a good approximation for a few electronvolt spread near the Fermi surface, then the integral in Eq. (4) may be done exactly, including the slit geometry; i.e.,

$$dN/dE_{\perp} \sim \{E_{\perp}^{1/2} \tan^2 \alpha \theta(-\varphi_{Ps} \cos^2 \alpha - E_{\perp}) + E_{\perp}^{-1/2} (-\varphi_{Ps} - E_{\perp}) \theta(-\varphi_{Ps} - E_{\perp}) \theta(E_{\perp} + \varphi_{Ps} \cos^2 \alpha)\} |\psi_i(\bar{z} + z_c)|^2_{E_i = E_F}. \quad (6)$$

Here  $\alpha$  is the collimator half-angle and  $\theta(x)$  is the unit step function.

The time-of-flight distribution  $S(z_0, t)$  can be related to the energy distribution  $dN/dE_{\perp}$  by integrating the time- and space-dependent distribution function (free streaming) over the collimator and the slit at  $z = z_0$ . We find that we may transform our data  $S$  to an energy distribution by multiplying by  $t^2$  and plotting it on an energy scale as shown in Fig. 4. Before making this transformation, the constant background from scattered orthopositronium-annihilation photons was subtracted from the time-of-flight data in Fig. 2. The curves in the figure are obtained from Eq. (6) after folding in the experimental time and spatial resolutions. For clean Al, the data points with  $E_{\perp} > 1.2 \text{ eV}$  are well

fitted by the theory (solid line in Figs. 2 and 4) with  $\varphi_{Ps} = -2.62 \pm 0.04 \text{ eV}$ . The value of  $\chi^2$  per degree of freedom for this fit is  $\chi^2/\nu = 158.3/98$  and the error bar has been doubled to take this into account. The plotted points are the average of pairs of data points. The measured positronium work function is in agreement with the prediction  $\varphi_{Ps} = -2.60 \pm 0.03 \text{ eV}$  obtained from independent measurements of  $\varphi_+$  and  $\varphi_-$ . The disagreement between theory and the clean-Al experiment for lower energies is attributed to contributions from scattered Ps. The  $O_2$ -exposed-Al data could only be fitted by Eq. (6) over a somewhat smaller range of energies,  $E_{\perp} > 1.7 \text{ eV}$  (see dashed curves in Figs. 2 and 4). Fixing  $\varphi_{Ps}$  at  $-2.62 \text{ eV}$  we obtained  $\chi^2/\nu = 151.8/75$ . The  $O_2$ -

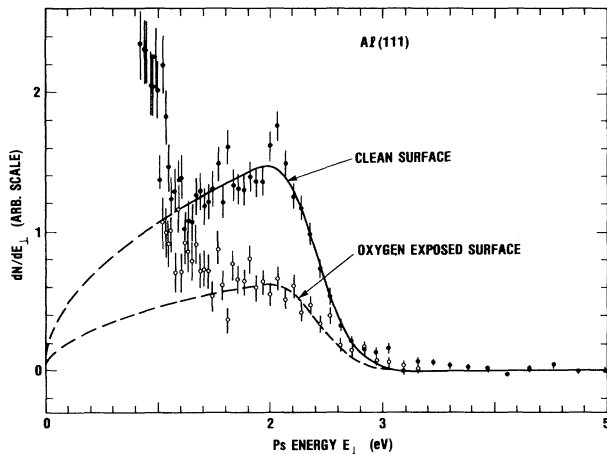


FIG. 4. Data of Fig. 2 replotted on an energy scale.

exposed-Al data show a much smaller break at the Fermi surface, in a way suggestive of the density-of-states calculation by Bylander, Kleinman, and Mednick.<sup>8</sup> These authors show that the Fermi-surface break is almost eliminated and that the bulk of the electron density is now concentrated in a peak located about 10 eV below the Fermi surface, implying that the magnitude of the wave function  $|\psi_j|^2$  for  $E_j$  in the neighborhood of  $E_F$  [see Eq. (6)] is strongly reduced.

The counting rates for low energies in Fig. 2 are about the same for the clean and  $O_2$ -exposed Al because the reduced background from scattered energetic Ps in the latter case is compensated by an increase in the low-energy part of the spectrum associated with the shift in the density of states toward lower energies. We also note that Lynn<sup>3</sup> observed an increase in the Ps yield of an  $O_2$ -exposed Al sample. The excess Ps that he observed has a very low kinetic energy ( $<0.25$  eV), as we have demonstrated in a separate series of measurements, and can be attributed to the spontaneous desorption of the surface positrons. The excess Ps is thus below the energy cutoff of our present experiment.

Surface states have been observed by angle-resolved photoemission experiments on clean Al surfaces.<sup>9</sup> These surface states occur at an energy accessible by our Ps-emission experiment, but have a value of  $k_{||}$  beyond the reach of our present collimator. It should be possible to improve the energy and angular resolution of our apparatus to investigate such surface states with a precision competitive with the photoemission data.<sup>10</sup>

In conclusion we note the following: (i) Meas-

urement of  $\varphi_{Ps}$  provides a precise characterization of a solid, which is expected to be free of the effects of surface crystallographic orientation, contamination, and charging. (ii) In combination with a measurement of  $\varphi_+$ ,  $\varphi_{Ps}$  provides a method for measuring  $\varphi_-$  with a precision at least equal to conventional methods. (iii) The data support a simple lowest-order picture of fast Ps emission, and suggest it is now possible to probe the density of states of more complicated metals. (iv) The use of polarized positrons<sup>11</sup> may allow mapping of the spin-dependent density of states at the surface of a ferromagnet. (v) Our model for the fast Ps formation process can be extended to describe formation of the positron surface state and slow positron emission. The formation of Ps and the surface state is associated with the production of electron-hole pairs and is in accord with the inelastic surface interaction model of Wilson.<sup>12</sup>

We are pleased to acknowledge helpful discussions with D. E. Gidley, C. A. Murray, M. C. Cardillo, and K. G. Lynn.

<sup>1</sup>K. F. Canter, A. P. Mills, Jr., and S. Berko, *Phys. Rev. Lett.* **33**, 7 (1974). For an extensive list of references see, for example, A. P. Mills, Jr., *Science* **218**, 335 (1982).

<sup>2</sup>A. P. Mills and L. N. Pfeiffer, *Phys. Rev. Lett.* **43**, 1961 (1979); D. W. Gidley, P. W. Zitzewitz, K. A. Marko, and A. Rich, *Phys. Rev. Lett.* **37**, 729 (1976).

<sup>3</sup>K. G. Lynn and H. Lutz, *Phys. Rev. B* **22**, 4143 (1980), and references therein.

<sup>4</sup>A. Held and S. Kahana, *Can. J. Phys.* **42**, 1908 (1964); H. Kanazawa, V. H. Ohtsuki, and S. Yanagawa, *Phys. Rev.* **138**, A1155 (1965); D. N. Lowy and A. D. Jackson, *Phys. Rev. B* **12**, 1689 (1975).

<sup>5</sup>N. D. Lang and W. Kohn, *Phys. Rev. B* **1**, 4550 (1970).

<sup>6</sup>H. Hagstrum, in *Electron and Ion Spectroscopy of Solids*, edited by L. Fiermans, T. Vennis, and W. Dekeyser (Plenum, New York, 1978); W. Sesselmann *et al.*, *Phys. Rev. Lett.* **50**, 446 (1983).

<sup>7</sup>G. F. Wertheim and P. H. Citrin, *Photoemission in Solids I*, edited by M. Cardona and L. Levy (Springer, Berlin, 1978).

<sup>8</sup>D. M. Bylander, L. Kleinman, and K. Mednick, *Phys. Rev. Lett.* **48**, 1544 (1982).

<sup>9</sup>G. V. Hamson and S. A. Flodstrom, *Phys. Rev. B* **18**, 1562 (1978). We would like to thank K. G. Lynn for bringing this reference to our attention.

<sup>10</sup>P. J. Schultz, K. G. Lynn, and W. E. Frieze (to be published) have obtained preliminary evidence for electron surface states in an experiment similar to ours.

<sup>11</sup>D. W. Gidley, A. R. Koymen, and T. W. Capehart, *Phys. Rev. Lett.* **49**, 1779 (1982).

<sup>12</sup>R. J. Wilson, *Phys. Rev. B* **27**, 6974 (1983).